Article

Radial imbibition in paper under temperature differences

A. López-Villa[1], A. Medina[1,2], F.J. Higuera[2], J.R. Mac Intyre[3], C.A. Perazzo[4] and J.M. Gomba[3]*

[1] ESIME Azcapotzalco, Instituto Politécnico Nacional, Av. de las Granjas 682 col. Santa Catarina,CDMX 02250, México.
[2] ETSI Aeronautica y del Espacio UPM, Plaza Cardenal Cisneros S/N, 28040 Madrid, Spain.
[3] Instituto de Física Arroyo Seco IFAS(UNCPBA) and CIFICEN (UNCPBA-CICPBA-CONICET), Pinto 399,7000, Tandil,Argentina.
[4] IMeTTyB, Universidad Favaloro-CONICET, Solís 453, C1078AAI Buenos Aires, Argentina.
* Correspondence: jgomba@engineering.ucsb.edu

Version April 27, 2019 submitted to Fluids

Abstract: Spontaneous radial imbibition into thin circular samples of porous material when they have been subjected to radial temperature differences was analyzed theoretically and experimentally. The use of the Darcy equation allows us to take into account temperature variations in the dynamic viscosity and surface tension in order to found the one-dimensional equation for the imbibition fronts. Experiments using blotting paper show a good fit between the experimental data and theoretical profiles through the estimation of a single parameter.

Keywords: Imbibition; Porous media; Thermocapillary phenomena

1. Introduction

The aim of this work is to study imbibition, *i.e.*, the spontaneous capillary penetration of a viscous liquid into a homogeneous, thin, circular, dry porous medium to which it has been imposed previously a temperature difference ΔT along the radial direction, r. Isothermal imbibition from an unlimited liquid reservoir has received attention due its important applications in paper chromatography [1,2], printing ink [3], paper absorption [1,4–6] and aerosol research [5,7]. In the latter case, the spreading of liquid drops into a porous substrate is of much interest because it corresponds to radial imbibition from finite liquid volumes [5,7,8].

Isothermal radial imbibition in horizontal porous samples has been studied, for example in samples of paper [1,5,6], in 3D cubical scaffold with cylindrical struts [8] and in thin Hele-Shaw cells filled with granular material [9]. Moreover, studies of radial imbibition in Hele-Shaw cells following a one-dimensional approach (without granular material) yield a similar equation for the advance front, as a function of time [4,10], as those reported for thin radial porous samples.

Imbibition to high temperature it is very frequent during enhanced oil recovery [11–13] and in soldering when non-reactive liquid metals are involved [14]. Mean temperatures around 400 K are typical during enhanced oil recovery while higher temperatures (450-2300 K) occur during welding with liquid metals. Temperature gradients also appear in both processes due to a non uniform heating. However, during imbibition under temperature gradients the viscous drag and the driven capillary force can change substantially because viscosity and surface tension are strongly dependent on temperature [12,14]. The main assumption in our treatment is that the temperature spatial variations ($T(\mathbf{x})$, where $\mathbf{x}$ is the position vector), in the absorbing medium, affect dynamic viscosity μ and surface tension σ. Moreover, in many liquids dynamic viscosity and surface tension decrease as temperature increases ($d\mu/dT$ and $d\sigma/dT < 0$), and during imbibition under temperature gradients both effects compete [15]. The manner in which the wet region advances, in a radial geometry, as time proceeds is the main subject of this work.

To establish the temperature gradient on the circular porous samples of small thickness e, we have imposed a temperature difference between the internal perimeter of a central orifice and the external perimeter of a metal circular plate upon the circular strips of paper rest on. This procedure allows us to have very controlled temperature gradients on the paper which is our porous medium of work.

To reach our goals, the division of this work is as follows. In the next section, we give the solution to the one-dimensional heat conduction problem in a solid impervious plate and in the absorbing medium. In Section 3, by using the solution of the conduction problem we treat the imbibition problem with temperature differences along a thin porous medium. There, the theoretical study of imbibition into porous media has been carried out by using the Darcy equation with viscosity dependent of temperature. In order to compare several cases, isotherm imbibition was also analyzed. In Section 4, a set of experiments in commercial blotting paper sheets, under temperature gradients, were made and a good fit of the theoretical profiles was obtained. Finally, Section 5 presents the main conclusions and remarks.

2. Temperature on circular plates

Lets us start the description of the heat conduction problem to establish the temperature difference $\Delta T = T_1 - T_0$ in an horizontal, thin impervious metal plate through the use of cylindrical coordinates (r, z, ϕ). The origin of this system is located at the center of the circular plate, as shown in Fig. 1, which has an orifice of radius R_0. The temperatures were fixed as T_0 in the inside perimeter of an orifice of diameter R_0 and T_1 along the outer perimeter of the circular plate of radius R_1. It allows to impose a steady-state temperature distribution only dependent on the radial coordinate r, $T = T(r)$, which can be obtained through the solution of the Laplace equation $\nabla^2 T = 0$ under the boundary conditions $T = T_0$ at $r = R_0$ and $T = T_1$ at $r = R_1$. The solution of the Laplace equation yields a temperature distribution of the form

$$T = T_0 + \frac{T_1 - T_0}{\ln R_1 - \ln R_0} (\ln r - \ln R_0), \quad (1)$$

and the temperature gradient $G = dT/dr$ is given by

$$G = \frac{T_1 - T_0}{\ln R_1 - \ln R_0} \frac{1}{r}, \quad (2)$$

notice that the temperature gradient is a function of r.

After the imposition of the temperature distribution on the horizontal metal plate we place upon it, very close together, a thin, circular porous sample of radii R_0 and R_1. Consequently, the porous medium acquires, by conduction, the same temperature distribution of the metal plate. Since the temperature difference $\Delta T = T_1 - T_0$ can be positive or negative, we have that the spatially averaged temperature gradient, $\overline{G}$, defined as

$$\overline{G} = \frac{\int_{R_0}^{R_1} G dr}{\int_{R_0}^{R_1} dr} = \frac{\Delta T}{(R_1 - R_0)}, \quad (3)$$

can be positive if $T_0 < T_1$ ($\Delta T > 0$, temperature increases when r increases) or negative if $T_0 > T_1$ ($\Delta T < 0$, temperature decreases when r increases).

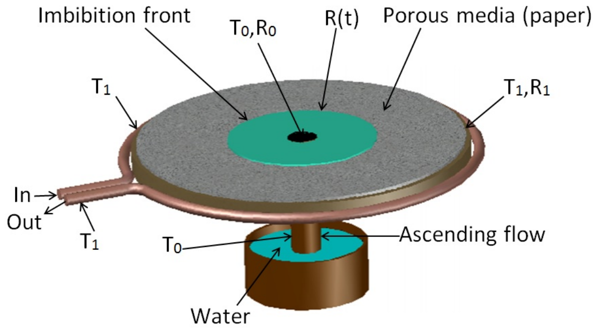

Figure 1. Schematic of the imbibition process in a thin paper on a circular copper plate. The paper sample has an inner radius R_0 and an outer radius R_1, and thickness e. Temperatures at $r = R_0$ and $r = R_1$ are T_0 and T_1, respectively. The blue sector indicates the imbibed region and the circular profile $r = R(t)$ indicates the instantaneous position of the imbibition front.

3. Imbibition into a porous medium

Isothermal imbibition into thin dry porous circular strips generates circular advance fronts of radius $r = R(t)$, where t is the elapsed time by the front to reach the radius R. At short time lapses, the front evolves as $R \propto t^{1/2}$ which is the Washburn diffusive law [16], and for long times, the imbibition front obeys a logarithmic relation which will be discussed afterwards.

Imbibition into the thin circular porous samples under temperature gradients is studied here by assuming that the saturation of the porous medium under imbibition is full, which is a simple and realistic approximation for thin samples. In our study we consider a sample of thin thickness e, outer radius $r = R_1$, an inner radius $r = R_0$ and it rests on the circular the metal circular plate having a radial temperature difference ΔT between their perimeters. Thus the temperature distribution on paper is the same as that given by Eq. (1) for the metal plate. In porous media, typically the Reynolds numbers during imbibition are low [17], thus the use of the Darcy equation is adequate here. Experimental observations given in the next section let us assume that radial imbibition under homogeneous temperature gradients will maintain purely radial fronts. Therefore, the one-dimensional Darcy equation for the filtration velocity, v_r, takes the form

$$v_r = -\frac{c_1 d^2}{\mu(r)} \frac{dp}{dr}, \tag{4}$$

where d is the pore diameter, c_1 is a lumped constant that involves the structure of the porous medium (in a general context the permeability of the porous media met that $K \sim d^2$ [18]), p is the pressure in the liquid and the term $\mu(r)$ specifies that the dynamic viscosity changes point to point where the liquid is present because temperature is non uniform.

When a liquid contacts a wettable porous medium it is imbibed spontaneously due to the pressure drop, $\Delta p = p_{atm} - p_c$, where p_{atm} is the atmospheric pressure, assumed as zero in this work, and p_c is the capillary pressure defined just at the imbibition front located at $r = R$. The surface tension takes the value $\sigma(r = R)$ because the existence of the temperature distribution in the porous medium yields, just on the front, a value that depends on temperature. Then, the pressure drop is the capillary pressure which induces the liquid motion into the porous medium

$$\Delta p = -\frac{c_2 \sigma(R)}{d}, \tag{5}$$

here, the new lumped constant c_2 is related to the structure of the porous medium, the inter-fibre and intra-fibre pores [19] and the contact angle between the liquid and the porous material which is assumed as non dependent on temperature for many liquids [20].

The integration of the Darcy equation (4) yields

$$\Delta p = -\int_{R_0}^{R} \frac{\mu(r) v_r}{c_1 d^2} dr, \tag{6}$$

where we have considered that the dynamic viscosity is a function of the temperature itself and temperature is a function of r.

When liquid loss due to evaporation from the porous media can be neglected, the mass conservation implies that $v_r = (R/r)dR/dt$ from which it follows, through the use of Eqs. (5) and (6), that

$$\frac{R}{d^2}\frac{dR}{dt}\int_{R_0}^{R} \frac{\mu(r)}{r} dr = \frac{c\sigma(R)}{d}, \tag{7}$$

being $c = c_1 c_2$.

Since a fundamental point of view the dynamic viscosity and the surface tension depend on temperature in a non linear form. However, computationally and experimentally, it has been proved that the use of linear approximations are valid in small ranges [13–15]. It allows to introduce linear laws for μ and σ such that $\mu(r) = \mu_0(1 + 1/\mu_0[(d\mu/dT)(dT/dr)]_{R_0}(r - R_0))$ and $\sigma(R) = \sigma_0(1 + 1/\sigma_0[(d\sigma/dT)(dT/dR)]_{R_0}(R - R_0))$, where μ_0 and σ_0 are the values of dynamic viscosity and surface tension at a reference temperature, $T = T_0$ where $r = R_0$. The substitution of the temperature gradient given in Eq. (2) into the previous relations yield

$$\mu(r) = \mu_0\left(1 + \frac{1}{\mu_0}\left(\frac{d\mu}{dT}\right)_{T_0}\frac{T_1 - T_0}{\ln[R_1/R_0]}\left[\frac{r}{R_0} - 1\right]\right), \tag{8}$$

$$\sigma(R) = \sigma_0\left(1 + \frac{1}{\sigma_0}\left(\frac{d\sigma}{dT}\right)_{T_0}\frac{T_1 - T_0}{\ln[R_1/R_0]}\left[\frac{R}{R_0} - 1\right]\right). \tag{9}$$

Using the linear relations (8) and (9) in Eq. (7) lets us found the motion equation in the form

$$\frac{\mu_0}{d^2}R\frac{dR}{dt}\left\{\ln\left(\frac{R}{R_0}\right) + \frac{1}{\mu_0}\left(\frac{d\mu}{dT}\right)_{T_0}\frac{T_1 - T_0}{\ln[R_1/R_0]}\left(\frac{R}{R_0} - 1 - \ln\frac{R}{R_0}\right)\right\} = \frac{c\sigma_0}{d}\left[1 + \frac{1}{\sigma_0}\left(\frac{d\sigma}{dT}\right)_{T_0}\frac{T_1 - T_0}{\ln[R_1/R_0]}\left(\frac{R}{R_0} - 1\right)\right]. \tag{10}$$

Through the introduction of the dimensionless radius $\xi = R/R_0$, the dimensionless time $\tau = t/t_c$, with the characteristic time t_c defined as

$$t_c = \frac{\mu_0 R_0^2}{c\sigma_0 d}, \tag{11}$$

and the dimensionless parameters

$$A = \frac{\left(\frac{d\mu}{dT}\right)_{T_0}[T_1 - T_0]}{\mu_0 \ln[R_1/R_0]}, \quad B = \frac{\left(\frac{d\sigma}{dT}\right)_{T_0}[T_1 - T_0]}{\sigma_0 \ln[R_1/R_0]}, \tag{12}$$

into Eq. (10), we found the dimensionless non linear differential equation for the imbibition front in the porous medium under a temperature gradient

$$\xi\frac{d\xi}{d\tau}\left[\ln\xi + A(\xi - 1 - \ln\xi)\right] = 1 + B(\xi - 1), \tag{13}$$

which will be solved using the initial condition $\xi = 1$ at $\tau = 0$. The solution of the differential equation (13) will be computed numerically in following Section.

In the context of the imbibition under temperature gradients the physical parameters of the problem t_c (Eq. (11)), A and B (Eq. (12)) have specific meanings: t_c is the viscous-capillary time indicating that the initial imbibition radius at $\tau = 0$ is finite [8] and it also involves the structure of the porous medium through d. A is the non dimensional relative variation of viscosity with temperature and B is the dimensionless relative variation of the surface tension with temperature. Later on we will notice the dynamical changes produced by A and B.

If imbibition occurs at uniform temperature, we have that $A = B = 0$. Clearly, the case of isothermal imbibition produces the dimensionless non linear differential equation $\xi(d\xi/d\tau)\ln\xi = 1$, its solution gives the non dimensional imbibition front, ξ, as

$$\xi^2\left(\ln\xi^2 - 1\right) + 1 = 4\tau. \tag{14}$$

For small dimensionless radius of imbibition ($\xi = 1 + \epsilon$, with $\epsilon \ll 1$), the asymptotic imbibition front now is given by

$$\xi = 1 + \sqrt{2\tau}, \tag{15}$$

which is the Washburn law for radial isotherm imbibition [6]. In the following Section we will discuss a set of experiments made in order to prove the validity of our model.

4. Experiments

The validity of our previous approach to dealing with the imbibition under temperature radial gradients will be analyzed here. To impose the gradients we used a circular copper plate $5 \times 10^{-3}\ m$ thickness, drilled at its center with an inner radius $R_0 = 2 \times 10^{-3}\ m$, and having an exterior radius $R_1 = 3.15\ \times 10^{-2}\ m$. The central orifice was joined to a copper vertical pipe of radius slightly smaller than $2 \times 10^{-3}\ m$ to get a good contact between the pipe and the plate (see Fig. 1). Additionally, the short pipe was brimful with dry sand and it also was in contact with a copper reservoir which was maintained at a temperature T_0. All these contacts allowed to have a temperature T_0 at $r = R_0$ in the copper plate. The external rim of the disk was surrounded by a copper pipe through which water was recirculated to maintain the external perimeter of the disk at an uniform temperature T_1, just at $r = R_1$. This array lets us to achieve controlled temperature gradients through the difference $\Delta T = T_1 - T_0$ between the internal and the external perimeters.

Once the steady temperature profile was reached on the copper disk, circular samples of blotting paper sheets $R_0 = 2 \times 10^{-3}\ m$ inner radius and $R_1 = 3.1\ \times 10^{-2}\ m$ outer radius were placed on the copper disk (having an hydrophobic coating to avoid wetting on it) in order to got by conduction exactly the same temperature profile as that of the disk itself, then, the imbibition is set in motion when the lower reservoir was filled with water and it rose trough the sand in the pipe up to the plate where sand, contacting circular samples of blotting paper by its inner rim, allowed the radial imbibition process.

To carry out the imbibition experiments we have selected commercial blotting paper as porous material because it is thin, $e = 3.1 \times 10^{-4}\ m$ average thickness. The nominal paper permeability in this case is 5 Darcy and consequently its average pore diameter is $d \sim \sqrt{K} \approx 2.23 \times 10^{-6}\ m$. When the dry blotting paper is placed on the copper disk the heat is diffused through the paper thickness allowing to establish the same temperature profile as that of the metal disk, this process involves a diffusion time given by $t_{Dp} = e^2/\alpha_p$ [23], where α_p is the thermal diffusivity of dry paper which has a value $\alpha_p = 8.7 \times 10^{-8}\ m^2/s$ [24], thus the approximate time it takes the dry paper to reach the temperature of the metal disk is $t_{Dp} = 1.1$ s.

Three values for the mean gradients were attained: a) case of a positive mean temperature gradient $T_0 = 301.4\ K$ (28.2 °C), $T_1 = 304.4\ K$ (31.2 °C), $\overline{G}_+ = 103.45\ K/m$, b) case of negative gradient $T_0 = 302.4\ K$ (29.2 °C), $T_1 = 299.4\ K$ (26.2 °C), $\overline{G}_- = -103.45\ K/m$, and c) the isotherm case with $\overline{G} = 0$ and temperature $T_0 = T_1 = 301.2\ K$ (28 °C). Note that we have chosen $\left|\overline{G}_-\right| = \overline{G}_+$ in order to have a direct comparison between cases with negative and positive gradients. The spatial temperature profiles were obtained by means of an infrared camera model Thermacam Flir PM595, with $\pm 2\ 0.1\ K$ of error in the measurement. Several representative profiles on the dry paper are shown in Fig. 2. In such a figure the plots on the right-hand side show the temperature profiles and their fluctuations are related to the measurement error which in this cases are around $\pm 0.1\ ^\circ C$.

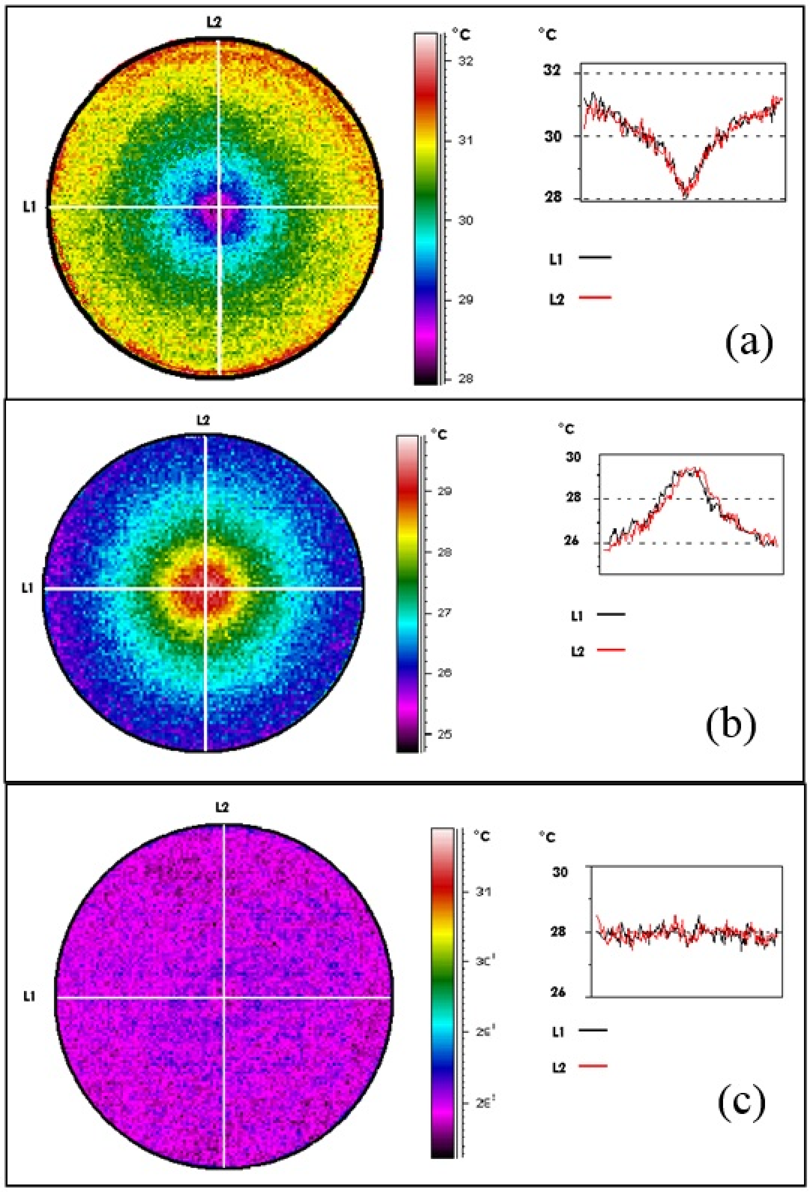

Figure 2. Temperature distribution on dry blotting paper for the several cases: (a) Upper figure: positive mean gradient, (b) Middle figure: negative mean gradient and (c) Lower figure: isothermal case. Thermographies are on the left-hand side meanwhile the measured temperature profiles are on the right-hand side. The respective profiles fit approximately Eq. (1). and fluctuations are related to the measurement error which in these cases are of around $\pm 0.1\ ^\circ C$.

When the temperature profiles have been imposed on the paper and the water imbibition occurs, we performed measurements of the radial imbibition fronts R as a function of time, t. In Fig. 3 the plot of R *vs* t is shown for the three temperature distributions (symbols).

We can compute the dimensionless factors A and B, for each respective case, from data for viscosity and water-air surface tension given in plots of Fig. 4 and the temperature distributions already established, we obtained that $A = -2.58 \times 10^{-2}$ and $B = -2.90 \times 10^{-3}$ for positive average gradient and $A = 2.61 \times 10^{-2}$ and $B = 2.91 \times 10^{-3}$ for negative average gradient. Notice that A is an order of magnitude larger than B, it means that the viscosity variation will produce stronger effects on the evolution of the imbibition fronts as temperature changes.

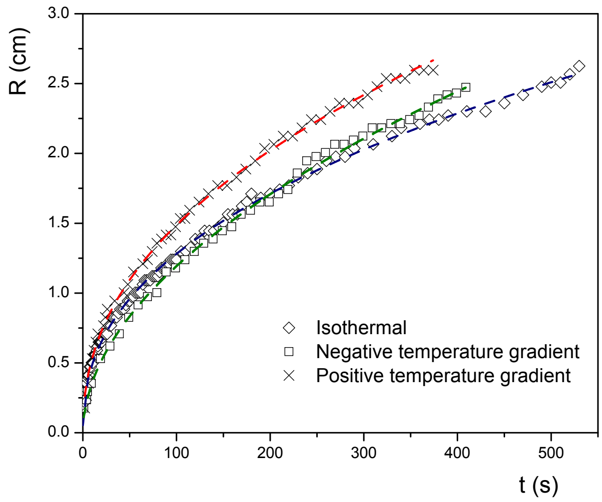

Figure 3. Dimensional plot of the time evolution of the experimental imbibition fronts (symbols) for positive and negative gradients and for the isotherm case where $T_0 = T_1 = 301.2\,K$ (28 °C). Dashed curves correspond to the respective numerical solutions: red dashed line for case $\overline{G} > 0$, green dashed line for $\overline{G} < 0$ and blue dashed line for $\overline{G} = 0$. Symbol sizes correspond to the standard deviation of 5 %.

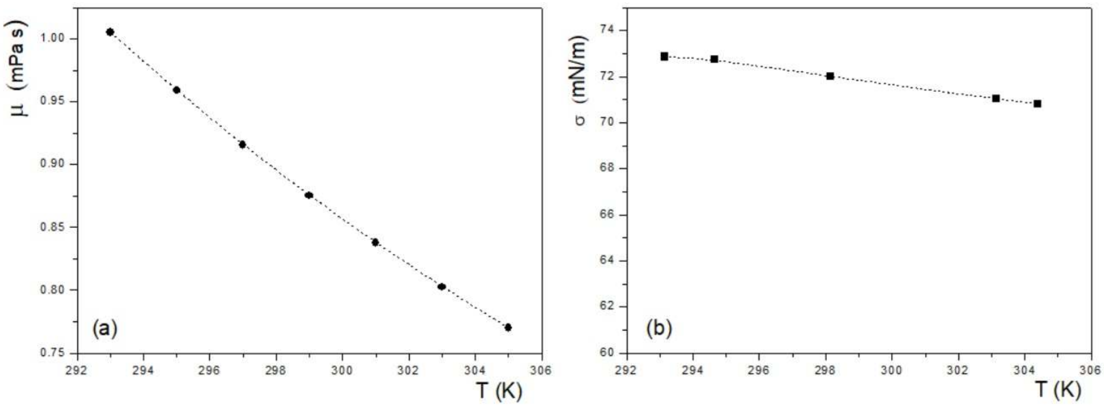

Figure 4. Plots of (a) dynamic viscosity of water and (b) water-air surface tension as a function of temperature. Data taken from [21,22].

The isotherm case is useful to show the effect of the temperature gradients on the evolution of the imbibition fronts but also this case lets us to determine the value of the lumped constant c as follows: the dimensional form of Eq. (15), which is valid for small radii R, has the form

$$R(t) = R_0 + \sqrt{\frac{2tc\sigma_0 d}{\mu_0}}, \tag{16}$$

by taking into account the corresponding experimental values of R_0, σ_0, μ_0, d and the time t, in such a formula we can obtain the theoretical data for $R(t)$. By correlating data for the theoretical $R(t)$ and the experimental data for R, at short times, given in plot of Fig. 3 for the isotherm case, we can obtain through the least squares method, that the best value for c is $c = 2.2 \times 10^{-3}$. This value was used to numerically compute the solution of Eq. (13) for positive and negative mean gradients and to compute the overall imbibition front for the isothermal case.

The numerical profiles (curves) fit satisfactorily the experimental data as is shown in Fig. 3. The non linear differential equation was solved numerically using a fourth order Runge-Kutta method, under the initial conditions described before.

The temporal changes on the imbibition fronts for each value of $\overline{G}$ are related to the respective values of A and B. From Fig. 3 it is clear that, at short times, the three curves follow approximately a behavior $R \sim t^{1/2}$ (Eq. (16)) but for later times the curves are separated between themselves. A more detailed behavior of the imbibition fronts can be shown more clearly in Fig. 5 where we plot the mean velocity of fronts as a time function. There, it is easily appreciated that for intermediate times velocity of each front is different but for larger times, again they are similar, *i.e.*, at intermediate times the relative changes for negative and positive gradients plays a different role between them but at large times these relative variations of viscosity and surface tension will vanished because far from $r = R_0$ the local gradients are weakest.

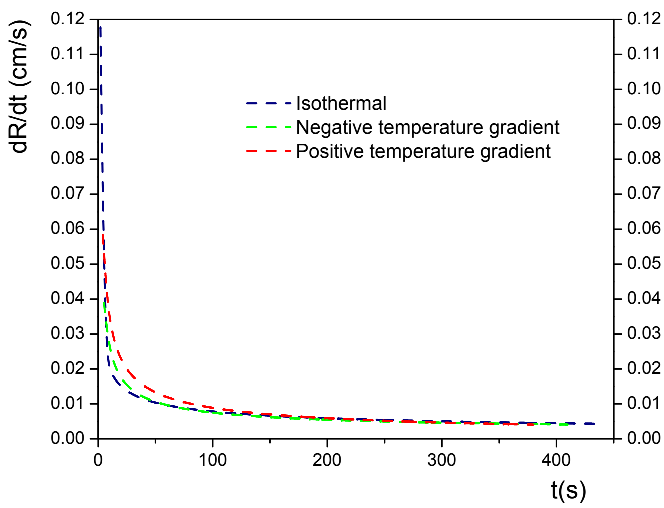

Figure 5. Plots of the averaged of velocity front as a function of time for the several mean gradients. Same data as in Fig. 3 were used.

Finally, it is important to comment that, generally speaking, the capillary penetration in the porous medium should be affected by the temperature, if the local temperature difference between the local bulk temperature of the liquid and the temperature of the most immediate grain or fiber can be neglected. This condition will be satisfied provided that the dimensionless relation $(dR/dt)\, d/\alpha_w \ll d_g/d$ is valid [23], where α_w is the liquid thermal diffusivity, d_g is the grain average diameter and d, as before, is the pore diameter. The quantity $(dR/dt)\, d/\alpha_w = Pe$ is the Peclet number and it compares the bulk transport of heat under forced convection (with velocity dR/dt) respect to the heat transfer by conduction. Thus, a very small Peclet number refers to a very slow flow where heat conduction dominates. Due to in blotting paper approximately $d \sim d_g$ we have that the condition $Pe \ll 1$ must be maintained for imbibition under temperature gradients. Consequently the imbibition model relies on these assumptions. In our case, experiments allows to estimate that for the initial times, where the front velocities are large, the Peclet number is $Pe \sim 0.018$ because for water $\alpha_w = 0.147 \times 10^{-2}$ cm^2/s (at room conditions) and thus our imbibition experiments fulfill this criterion. At the end, when each experiment was completed, we verified that approximately the respective temperature profiles (as those thermographies given in Fig. 2 for dry paper) in the imbibed papers are the same. It was occurred, effectively.

5. Conclusions

In this work we have studied both theoretically and experimentally the radial imbibition in thin samples of blotting paper. We show that spatial temperature differences induce important changes in the water viscosity and in the water-air surface tension which finally modify the time evolution of the imbibition fronts with respect to isothermal imbibition. Moreover, the simple theoretical model developed here to describe imbibition into a porous medium (blotting paper) with radial geometry is consistent with our present experimental results. It appears, despite the complexity of the phenomenon, that a simple, one-dimensional model can describe the main facts involved when there is not an uniform temperature.

Acknowledgments: One of us (A. M.) acknowledges partial support from Fondo SENER-Hidrocarburos, CONACYT for a stay at the UPM through the project *Fundamental models of the thermal methods of steam injection in EOR*. He also acknowledges to COTEBAL-IPN for a research annual leave. J.R.M.C, C.A.P. and J.M.G. acknowledges SPU, CICPBA and CONICET.

References

1. Muller, R.H.; Clegg, D.L. Physical and geometric factors. *Annal. Chem*. **1951**, *23*, 403-408.
2. Gillespie, T. The capillary rise of a liquid in a vertical strip of filter paper. *J. Colloid Sci.* **1959**, *14*, 123-130.
3. Ridgeway, C.J.; Gane, P.A.C. Controlling the absorption dynamic of water-based ink into porous pigmented coating structures to enhance print performance. *Nord. Pulp Paper Res. J.* **2002**, *17*, 119-129.
4. Marmur, A. The radial capillary. *J. Colloid Interface Sci.* **1988**, *124*, 301-308.
5. Danino, D.; Marmur, A. Radial capillary penetration into paper: limited and unlimited liquid reservoirs. *J. Colloid Interface Sci.* **1994**, *166*, 245-250.
6. Medina, A.; Pérez-Rosales, C.; Pineda, A.; Higuera, F.J. Imbibition in pieces of paper with different shapes. *Rev. Mex. Fis.* **2001**, *47*, 537-541.
7. Starov, V.M.; Kostvintsev, S.R.; Sobolev, V.D.; Velarde, M.G.; Zhdanov, S.A. Spreading of liquid drops over dry porous layers: complete wetting case. *J. Colloid. Interface Sci.* **2002**, *252*, 397-408.
8. Das, S; Milacic, E; Deen, N.G; Kuipers, J.A.M. Droplet spreading and capillary imbibition in a porous medium: A coupled IB-VOF method based numerical study. *Phys. Fluids* **2018**, *30*, 012112.
9. Chen, Y-J; Watanabe, S.; Yoshikawa, K. Roughening dynamics of radial imbibition in a porous medium. *Phys. Chem. C* **2015**, *119*, 12508
10. Middleman, S. *Modeling Axisymmetric Flows*; Academic Press: San Diego, 1995.
11. Babadagli, T. Temperature effect on heavy-oil recovery by imbibition in fractured reservoirs. *J. Pet. Sci. Eng.* **1996**, *14*, 197-208.
12. Morrow, N.R.; Mason, G. Recovery of oil by spontaneous imbibitions. *Current Opinion Colloid and Interface Sci.* **2001**, *6*, 321-337.
13. Amadu, M; Pegg, M.J. Analytical solution to spontaneous imbibition under vertical temperature gradient based on the theory of spontaneous imbibition dynamics, *J. Petr. Sci. Eng.* **2019**, *172*, 627–635.
14. Eastathopoulos, N. Nicholas, M.G, Devret, B. *Wettability at High Temperatures*; Pergamon Materials Series vol 3, Elsevier, Oxford, Uk, 1999.
15. Medina, A.; Pineda, A.; Treviño, C. Imbibition driven by a temperature gradient. *J. Phys. Soc. Japan* **2003**, *72*, 979-982.
16. Washburn, E.W. The dynamics of capillary flow. *Phys. Rev.* **1921**, *17*, 273-283.
17. Bear, J. *Dynamics of Fluids in Porous Media*; Dover: New York, 1988.
18. Dees, P.J.; Tjan, T.G.; Polderman, J. Determination of pore diameter by permeability measurements. *Powder Techol.* **1980**, *27*, 29-36.
19. Chang, S.; Seo, J.; Hong, S.; Lee D-G.; Kim, W. Dynamics of liquid imbibition through paper with intra-fibre pores. *J. Fluid Mech.* **2018**, *845*, 36-50.

20. Gomba, J.M.; Homsy, G.M. Regimes of thermocapillary migration of droplets under partial wetting conditions. *J. Fluid Mech.* **2010**, *647*, 125–142.
21. Dortmund data bank: http://ddbonline.ddbst.de/VogelCalculation/VogelCalculationCGI.exe?component=Water
22. Pallas, N.R.; Harrison, Y. An automated drop shape apparatus and the surface tension of pure water. *Colloids and Surf.* **1990**, *43*, 169-194.
23. Incropera, F.P.; Dewitt, D.P. *Fundamentals of Heat and Mass Transfer*; Wiley: New Jersey, 2002.
24. Lavrykov, S.A.; Ramarao, B.V. Thermal properties of copy paper sheets, *Drying Tech.* **2012**, *30*, 297-311.